ANNUAL REVIEWS

Annual Review of Neuroscience

Early Binaural Hearing: The Comparison of Temporal Differences at the Two Ears

Philip X. Joris[1] and Marcel van der Heijden[2]

[1]Department of Neurosciences, KU Leuven, 3000 Leuven, Belgium;
email: Philip.Joris@kuleuven.be

[2]Department of Neuroscience, Erasmus University Medical Center, 3000 CA Rotterdam, Netherlands

Annu. Rev. Neurosci. 2019. 42:433–57

First published as a Review in Advance on
April 24, 2019

The *Annual Review of Neuroscience* is online at
neuro.annualreviews.org

https://doi.org/10.1146/annurev-neuro-080317-061925

Keywords

hearing, stereo, coincidence detection, temporal processing, brainstem, sound localization

Abstract

Many mammals, including humans, are exquisitely sensitive to tiny time differences between sounds at the two ears. These interaural time differences are an important source of information for sound detection, for sound localization in space, and for environmental awareness. Two brainstem circuits are involved in the initial temporal comparisons between the ears, centered on the medial and lateral superior olive. Cells in these nuclei, as well as their afferents, display a large number of striking physiological and anatomical specializations to enable submillisecond sensitivity. As such, they provide an important model system to study temporal processing in the central nervous system. We review the progress that has been made in characterizing these primary binaural circuits as well as the variety of mechanisms that have been proposed to underlie their function.

Contents

1. GENERAL INTRODUCTION 434
2. TEMPORAL CUES AVAILABLE TO THE CENTRAL NERVOUS SYSTEM 434
3. USEFULNESS OF INTERAURAL TIMING CUES 436
4. BEHAVIORAL LIMITS 437
   4.1. Sensitivity to Interaural Time Differences 437
   4.2. Binaural Detection and Interaural Time Differences 437
   4.3. Nonhuman 439
5. CIRCUIT COMPONENTS 439
   5.1. Medial Superior Olive Circuit 440
   5.2. Lateral Superior Olive Circuit 441
6. MONAURAL PREPROCESSING 441
7. OUTPUT OF THE SUPERIOR OLIVARY COMPLEX 443
   7.1. Forms of Interaural Time Difference Sensitivity to Ongoing Sound 443
   7.2. Distribution of Best Delays 445
8. MECHANISMS OF SENSITIVITY TO INTERAURAL TIME DIFFERENCE 446
   8.1. Internal Delay 446
   8.2. Coincidence Detection in the Medial Superior Olive 448
9. THE LATERAL SUPERIOR OLIVE AS A COMPLEMENTARY INTERAURAL TIME DIFFERENCE PROCESSOR 450
10. SUMMARY AND OUTLOOK 450

1. GENERAL INTRODUCTION

Comparisons between receptors in different positions on the body can inform the brain regarding external space. Prominent examples are paired sense organs, particularly the eyes and ears. Investigation of the neural processing exploiting such pairing—or stereo—is attractive for several reasons. Stereo systems can be isolated behaviorally or physiologically: Random-dot stereograms reveal objects when viewed binocularly but appear featureless monocularly (Julesz 1971), and some signals can be heard binaurally but not monaurally (Hirsh 1948, Licklider 1948). Stereo systems obviously require convergence from paired sensors onto single neurons, which facilitates identification of the relevant circuits. An appeal of auditory stereo is that the main cue consists of tiny time differences between the ears, making binaural hearing a model system to study temporal processing. Here, we review the initial processing of interaural temporal differences at the level of the brainstem.

2. TEMPORAL CUES AVAILABLE TO THE CENTRAL NERVOUS SYSTEM

Binaural: combining the information from the two ears

In mammals, binaural hearing relies on central nervous system (CNS) mechanisms comparing sound-evoked neural events from the two ears. These events reflect the waveform of the physical stimuli as modified by the cochlea and nervous system. As the auditory nerve (AN) is the bottleneck feeding the CNS, we first consider the transformation of sound waves to AN action potentials (**Figure 1**).

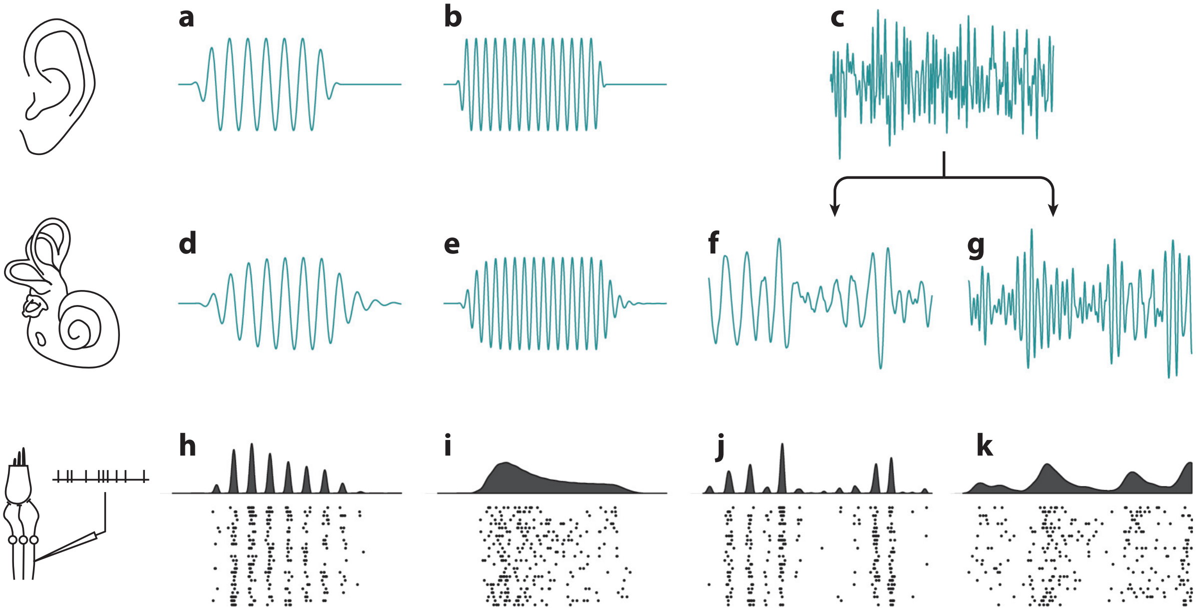

Figure 1

Schematic illustration of the transformation from sound waveforms to neural excitation. (*Top row*) Sound waveforms of (*a*) a low-frequency tone, (*b*) a high-frequency tone, and (*c*) wideband noise. (*Middle row*) The corresponding waveforms filtered by the cochlea: (*d*,*e*) low- and high-frequency tones at their own characteristic cochlear place and (*f*,*g*) the same wideband noise at apical and basal cochlear positions, respectively. (*Bottom row*) The timing of action potentials in the auditory nerve (AN) shown in (*top*) peri-stimulus time histograms and (*bottom*) corresponding dot rasters. The dots represent the timing of action potentials evoked by repeated presentations of the stimuli in the panel above. Responses to low frequencies (*h*,*j*) show fine structure (i.e., phase locking), while the responses to high frequencies (*i*,*k*) only show envelope coding.

The first major step is the spectral analysis by the cochlea, which decomposes sound into frequency bands. For narrowband sounds such as tones, this filtering has only minor effects (e.g., prolonged ringing after the tone ends) (**Figure 1*d*,*e***). Wideband noise, on the other hand, is completely transformed into a waveform with fairly regular zero crossings and a slowly fluctuating magnitude (i.e., envelope). The same wideband noise (**Figure 1*c***) gives rise to entirely different filtered waveforms (**Figure 1*f*,*g***) depending on the characteristic frequency (CF) of the cochlear site.

The second major step is transduction into action potentials. Importantly, nerve responses to low-frequency sounds (**Figure 1*h*,*j***) reflect the fine structure of the waveform, while responses to high frequencies only reflect slower envelope fluctuations (**Figure 1*i*,*k***). This limitation in temporal coding, expressed in terms of the phase locking limit (typically about 3–5 kHz) (Johnson 1980, Rose et al. 1967, Weiss & Rose 1988), has major implications on binaural processing. Lord Rayleigh's duplex theory stated that low- and high-frequency sounds are localized based on their interaural time delays (ITDs) and interaural level differences (ILDs), respectively (Lord Rayleigh 1907). This view is no longer accepted, as high-frequency ITDs do contribute to localization and binaural detection (McFadden & Pasanen 1976). But the use of high-frequency ITDs critically depends on the presence of sharp on- and offsets or pronounced envelope fluctuations. Even if present, these cues are easily spoiled by background noise and reverberation. In comparison, the information carried by the temporal fine structure of low-frequency sounds is more robust (Devore & Delgutte 2010) and generally more accurate (Bernstein 2001).

Envelope: hull of a waveform that tracks its intensity fluctuations on a timescale of multiple cycles

Characteristic frequency (CF): stimulus frequency to which an auditory neuron is most sensitive

Fine structure: finest temporal details of a waveform at the scale of individual cycles

Phase locking: a neuron's ability to code fine structure

3. USEFULNESS OF INTERAURAL TIMING CUES

Interaural time delay (ITD): arrival time difference of a sound at the two ears, depending on angle of incidence

A basic use of ITDs is the localization of a single sound source in a silent, anechoic environment. The ITD varies with azimuth, and its maximum value is determined by headwidth, the distance between the ears, which is an important variable between species. The headwidth of humans corresponds to a maximum ITD of approximately 750 µs. In daily life, however, idealized static ITD estimation is rare. The sound waveforms at the two ears are rarely simple delayed copies of each other. Different components of complex sounds acquire different, frequency-specific ITDs when reaching the ears (**Figure 2*a***). In the presence of competing sound sources or multiple

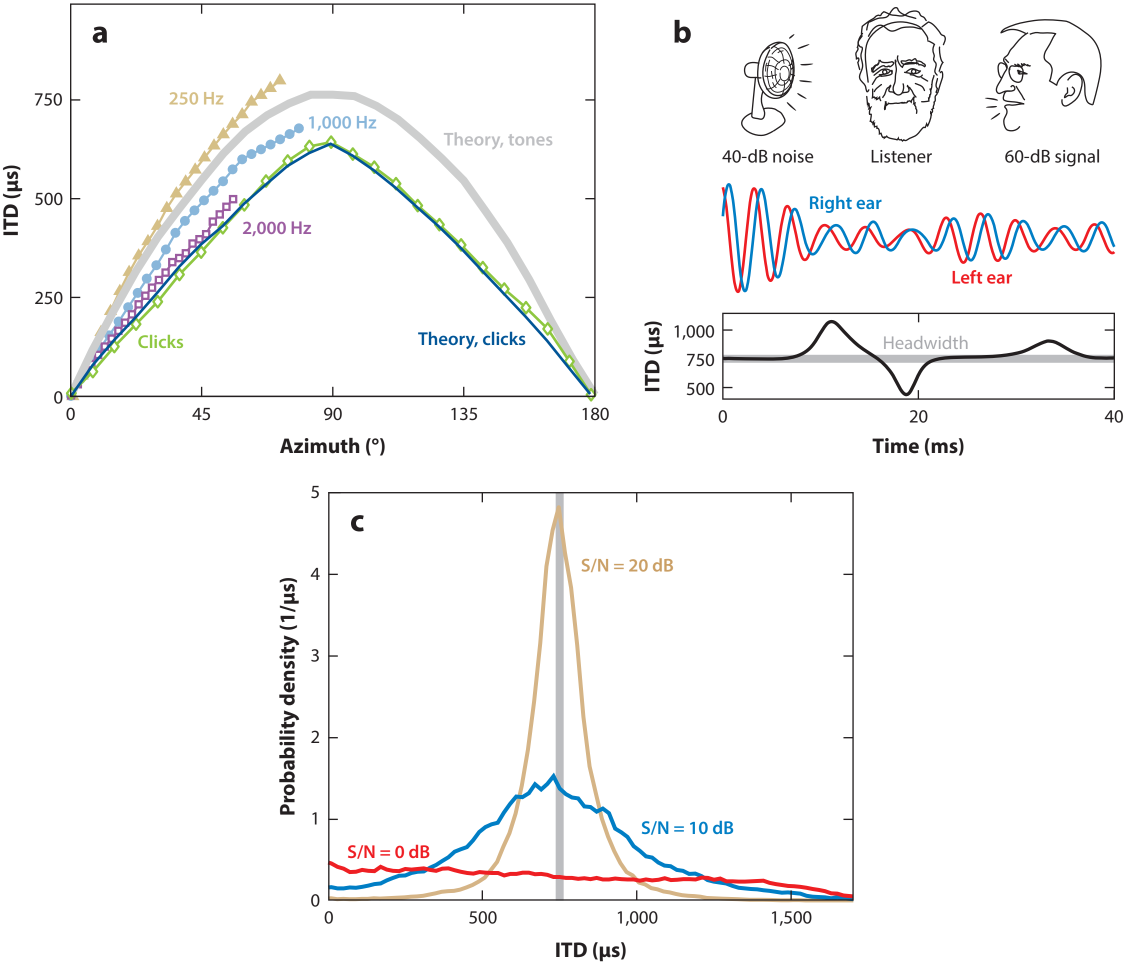

Figure 2

Interaural time delay (ITD) is not a straightforward localization cue. (*a*) The ITD depends on azimuth and also on frequency, causing the components of one complex sound to attain different ITDs. Panel *a* adapted from Durlach & Colburn (1978). (*b*) Competing sound sources cause the ITD to fluctuate in time. Two sources occur in free field at either side of the listener's head (±90°). The signal (near the left ear) is 20 dB above the noise (near the right ear). A representative snippet of the resulting waveforms at the two ears (middle) is shown, together with its instantaneous time-varying ITD (*bottom*). Note the excursions of ITD well exceeding the headwidth (*gray line*). (*c*) The statistical distribution of short-term ITD as in panel *b* for three signal-to-noise ratios is shown. (*b*,*c*) Signal and noise were 100-Hz-wide noise bands centered at 300 Hz.

acoustic paths produced by reverberation, their interference causes ITDs to fluctuate in time and to transiently exceed the headwidth, even when one of the sources is dominant (**Figure 2*b*,*c***).

These complications are not mere confounders of idealized waveform ITDs: The CNS processes and exploits this dynamic ITD information. The binaural system is thus much more than a simple ITD meter. Apart from single-source localization, binaural processing enhances source detection and identification. It also helps assess the acoustic properties of the environment and judge the reliability of available acoustic cues.

Interaural level difference (ILD): sound level difference between the ears caused by acoustic head shadow

Masking: one sound becoming inaudible due to the presence of another

4. BEHAVIORAL LIMITS

There is a rich history of binaural psychophysics in human listeners, ranging from headphone studies to free-field experiments and virtual reality (reviewed in Bernstein 2001, Durlach & Colburn 1978, Middlebrooks & Green 1991). We restrict our discussion to a few topics that have a close relationship to binaural physiology.

4.1. Sensitivity to Interaural Time Differences

Headphones allow the delivery of waveforms that are identical except for an interaural delay. In the low-frequency range, human listeners are extremely sensitive to such pure ITDs, requiring only a few microseconds for detection (Klumpp & Eady 1956). Free-field experiments are consistent with this finding. For low-frequency tones, the sensitivity to changing the angle of the loudspeaker from the midline amounts to only a few degrees, corresponding to an ITD change of approximately 10 μs (Mills 1958). When using a nonzero ITD (or a nonzero azimuth <60°) for the baseline condition, sensitivity drops somewhat, but not dramatically. Thus, humans do not have a pronounced binaural fovea. The exquisite sensitivity to ITDs at low frequencies is based on the fine structure of the ongoing portion of the sound and does not require marked onsets, offsets, or a fluctuating envelope. ITD sensitivity at low frequencies is much reduced when using artificial stimuli in which the envelope ITD is varied while keeping the fine structure fixed (Henning 1980) (**Figure 3*b***).

For high frequencies (>1,500 Hz), the situation is essentially reversed; the sensitivity to fine structure cues entirely disappears. A striking demonstration of the contrasting phase sensitivity at low and high frequencies is provided by binaural beats (**Figure 3*d***). Because of the high-frequency phase deafness, ITDs of high-frequency sounds can only be perceived through a fluctuating envelope (Henning 1974) (**Figure 3*b***) or on- and offsets (i.e., gating) (**Figure 3*c***). However, the sensitivity to ongoing envelope ITDs of high-frequency stimuli is 2–10 times poorer than sensitivity to ITDs in the fine structure at low frequencies (Bernstein 2001), and it degrades when the modulation depth is reduced (Nuetzel & Hafter 1981), e.g., as a result of reverberation (Houtgast & Steeneken 1985). In reverberant conditions, the only useful high-frequency ITD cue remaining is the direct field portion of sharp onsets, which arrives before any echoes do. Indeed, the earliest portion of waveforms is known to dominate the perceived lateral position (Wallach et al. 1949).

4.2. Binaural Detection and Interaural Time Differences

Auditory masking refers to soft signals becoming inaudible in the presence of noise. Masking can be partially undone by exploiting binaural information. If signal and masker differ in their interaural attributes, the signal's audibility is often enhanced. In a classical headphone study (Hirsh 1948, Licklider 1948), listeners detect tones presented with opposite polarity (antiphasically) to the two ears in the presence of diotic (interaurally identical) wideband noise (**Figure 4**). Presenting

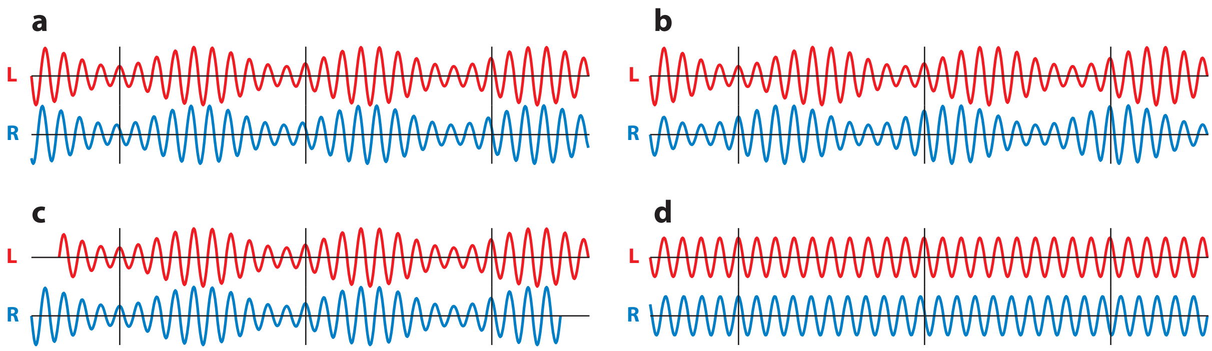

Figure 3

Different types of ITD cues in human psychophysics. Aspects of ITDs that always occur together in natural conditions can be teased apart using artificial stimuli: (*a*) ongoing ITDs in the fine structure, (*b*) ongoing ITDs in the envelope, and (*c*) onset and offset ITDs. Relative sensitivity to different ITD types is strongly frequency dependent: Fine-structure ITD dominates at low frequencies but becomes imperceivable above 1,500 Hz. ITD types in panels *a–c* are illustrated using amplitude-modulated tones, but they also apply to other stimuli. (*d*) Binaural beats provide a striking demonstration of the frequency dependence of binaural fine structure cues. Two tones of slightly differing frequency are presented to the two ears, causing a running interaural phase difference, the audibility of which depends on the carrier frequencies of the tones. When listening over headphones, they evoke a periodically varying spatial percept with low-frequency tones (e.g., 500/508 Hz; **Supplemental Audio 1**) but not with high-frequency tones (e.g., 2,000/2,008 Hz; **Supplemental Audio 2**). Abbreviations: ITD, interaural time delay; L, left; R, right.

low-frequency tones antiphasically (**Figure 4*b***) enhances their audibility by about 13 dB compared to presenting them identically (**Figure 4*a***). This phase reversal trick was applied to improve radio communication in noisy airplanes. Binaural unmasking is likely to play a role in everyday situations where signal and noise sources are at different spatial locations.

Adding the soft antiphasic tone to the noise masker introduces interaural disparities in the stimulus, which, after peripheral filtering, include the type of time-varying ITDs illustrated in **Figure 2*b***. Neural circuits with exquisite sensitivity to static ITDs also sense dynamically varying ITDs (Joris 2019, Joris et al. 2006c), making them well-suited to realize binaural unmasking and detect minute interaural decorrelation (Coffey et al. 2006, Louage et al. 2006, Shackleton et al. 2005). There is psychophysical evidence that dynamic ITDs are indeed the major cue for

Interaural decorrelation: deviation from the perfect statistical correlation ($\rho = 1$) of the waveforms entering the two ears

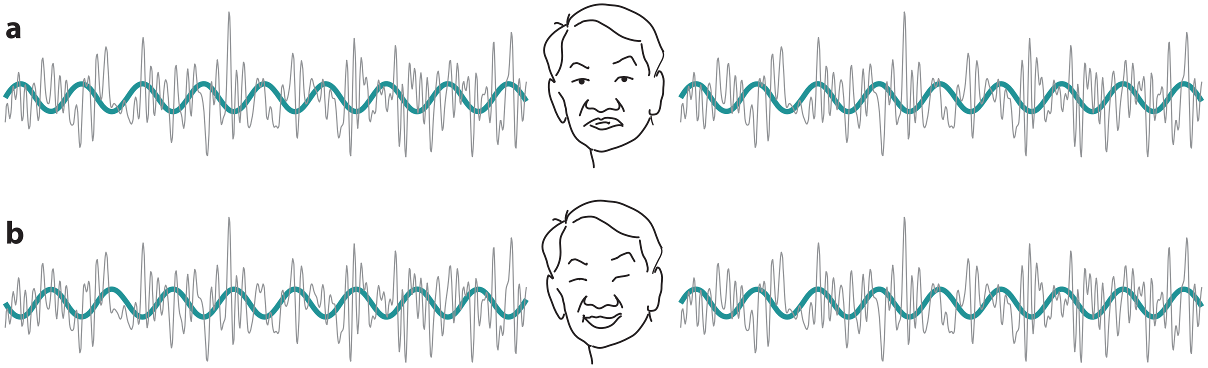

Figure 4

Binaural unmasking of a tone in noise. (*a*) The listener is unable to detect a soft tone (*green wave*, scaled up sevenfold) in the presence of a noise masker (*gray wave*) when noise and tone waveforms are presented to the two ears with identical polarity. (*b*) When the tone but not the noise masker is presented antiphasically (polarity-reversed in one ear), it becomes audible (**Supplemental Audios 3 and 4**).

detecting low-frequency tones in wideband noise (van der Heijden & Joris 2010). The importance of dynamic ITD processing is also consistent with the decline of binaural unmasking and correlation detection above 1,500 Hz, the same frequency limit observed for tonal ITDs and binaural beats (**Figure 3*d***). As illustrated in **Figure 2**, larger-than-headwidth ITDs are expected to play a role as the interference between signal and noise leads to occasional interaural phase opposition, creating a short-term ITD of half the signal period, i.e., up to several milliseconds. If the binaural system is to exploit these large excursions, it needs sensitivity to ITDs well beyond the headwidth limit. Indeed, larger-than-headwidth ITDs do lead to continued lateralization (Blodgett et al. 1956) and are likely to contribute to binaural unmasking (van der Heijden & Trahiotis 1999).

There is another fundamental link between binaural detection and ITDs. Performance in binaural detection is relatively insensitive to overall interaural delays of the entire stimulus, i.e., signal and noise together (Bernstein & Trahiotis 2018). This robustness against overall delays resembles the absence of a clear binaural fovea for ITD discrimination mentioned above. It suggests that the binaural processor has access to a repertoire of internal delays to compensate external delays in the stimulus (i.e., ITDs). Such a range of internal delays was first proposed by Jeffress (1948) and is a key attribute of most binaural models (Colburn & Durlach 1978, Durlach 1972, Stern et al. 1988). Experimental evidence (van der Heijden & Trahiotis 1999) indicates the use of internal delays of up to 2–3 ms, much larger than the approximately 750-μs headwidth limit of humans. The best delays (BDs) of binaural neurons (described below) can be viewed as the physiological counterpart to the internal delays of binaural psychophysics.

Internal delay: difference in delay at which the left and right ears affect a binaural neuron

Best delay (BD): the stimulus interaural time delay that optimally excites a binaural neuron

Superior olivary complex (SOC): an amalgam of brainstem nuclei also containing the neurons of primary binaural interaction

To summarize, in a limited view of the binaural system as a single-source ITD meter, the occurrence of cells tuned to larger-than-headwidth ITDs is something that needs special explanation (e.g., McAlpine et al. 2001). But in everyday situations involving competing sound sources, reverberation, and so on, the headwidth ceases to be the natural limit of ITD processing.

4.3. Nonhuman

The ability to localize and detect prey or predators is one of the major functions of hearing. Sound localization of free-field stimuli has been studied extensively in many mammalian species (reviewed in Brown & May 2005). Dichotic studies are technically challenging and few in number (B.H. Scott et al. 2007, Tolnai et al. 2018, Wakeford & Robinson 1974), but basic capabilities of binaural detection and ITD sensitivity have been documented. A general comparative theme has been to relate behavioral abilities to various anatomical features such as head size and brainstem anatomy. Importantly, some species (e.g., mice, rats) do not have low-frequency hearing. The main animal models to study ITD sensitivity are rodents with large middle ear spaces (e.g., gerbil, guinea pig, chinchilla) and other species with good low-frequency hearing (e.g., cat, rabbit, macaque).

5. CIRCUIT COMPONENTS

Initial binaural interactions occur in two brainstem circuits (**Figure 5**) centered on the medial superior olive (MSO) and lateral superior olive (LSO). These nuclei are embedded in the superior olivary complex (SOC) and share several input sources, which display remarkable physiological and anatomical specializations (see the sidebar titled Giant Synapses). There is marked variation in the absolute and relative size of SOC nuclei across species, including primates (Moore & Moore 1971), and covariation with other characters (Harrison & Irving 1966, Heffner & Heffner 1992, Masterton et al. 1975).

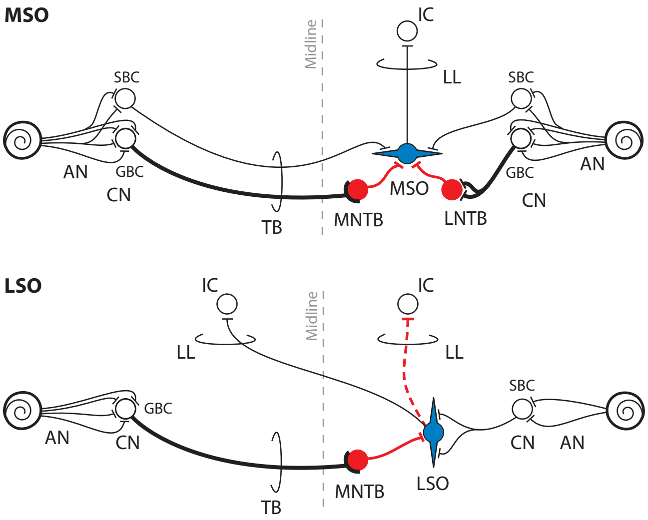

Figure 5

The two primary circuits of binaural interaction. TB and LL are fiber tracts, with inhibitory projections (*red*) and excitatory projections (*black*) indicated. The projection of the LSO to the ipsilateral IC is predominantly inhibitory (*red dashed line*). Abbreviations: AN, auditory nerve; CN, cochlear nucleus; GBC; globular bushy cell; IC, inferior colliculus; LL, lateral lemniscus; LNTB, lateral nucleus of the trapezoid body; LSO, lateral superior olive; MNTB, medial nucleus of the trapezoid body; MSO; medial superior olive; SBC, spherical bushy cell; TB, trapezoid body.

GIANT SYNAPSES

The monaural neurons providing excitation and inhibition to the medial and lateral superior olive receive limited convergence of inputs via large axosomatic terminals. This is particularly striking for spherical bushy cell (SBC), globular bushy cell (GBC), and medial nucleus of the trapezoid body (MNTB) neurons, which have similar morphology with a compact, bushy dendritic tree. We group them as bushy-type neurons. SBCs and GBCs receive nerve input via the end bulbs and modified end bulbs of Held, respectively. MNTB principal cells are monoinnervated by GBCs via the calyx of Held, one of the largest synapses in the brain.

5.1. Medial Superior Olive Circuit

The MSO is a striking elongated nucleus, a book-shaped slab only a few cells wide. Early studies (Ramón y Cajal 1909, Stotler 1953) drew attention to the bipolar morphology of its principal neurons, which show two main thick and branching dendrites oriented in opposite directions (Rautenberg et al. 2009, Smith 1995). The bipolar morphology enables the dendritic segregation of excitatory inputs from spherical bushy cells (SBCs), which branch to supply lateral MSO dendrites ipsilaterally and medial dendrites contralaterally (Beckius et al. 1999, Cant & Casseday 1986, Smith et al. 1993). Monaural sounds typically evoke low response rates from MSO neurons, which are labeled EE, for excited by contra- and ipsilateral ear. There is a tonotopic gradient along the MSO dorsoventral axis with an underrepresentation of high frequencies (Franken et al. 2015, Guinan et al. 1972, Karino et al. 2011). Whether there is also a rostrocaudal functional gradient has been a topic of considerable interest, discussed below.

Spherical bushy cell (SBC): projection neurons in the cochlear nucleus providing the main excitatory input to binaural superior olivary complex neurons

MSO neurons also receive inhibitory input, which provides a second path of binaural convergence. Glycinergic terminals cluster on their soma (Clark 1969, Kapfer et al. 2002). Globular bushy cells (GBCs) provide axosomatic terminals to two glycinergic nuclei projecting to the MSO: the posteroventral lateral nucleus of the trapezoid body ipsilaterally and the medial nucleus of the trapezoid body (MNTB) contralaterally (Banks & Smith 1992; Cant & Hyson 1992; Franken et al. 2016a; Kuwabara & Zook 1992; Roberts et al. 2014; Smith et al. 1991, 1998; Spangler et al. 1985; Spirou & Berrebi 1996, 1997; Spirou et al. 1990).

Globular bushy cell (GBC): projection neurons in the cochlear nucleus that excite superior olivary complex nuclei that are inhibitory to binaural neurons

Trapezoid body (TB): main output pathway of the part of the cochlear nucleus that contains bushy cell axons

Vector strength: metric for the degree of phase locking

5.2. Lateral Superior Olive Circuit

The LSO is an S-shaped nucleus that is lateral to the MSO. Here, the inputs from the two ears are opposite in sign but not segregated to different dendrites. Ipsilateral inputs are excitatory and occur dominantly on distal dendrites. Excitatory inputs are mostly derived from SBCs [at least partly the same SBCs also projecting to the MSO (Shneiderman & Henkel 1985, Smith et al. 1993)]. Inhibitory inputs derive from the homolateral MNTB and dominate on the LSO somata and proximal dendrites (Cant 1984, Cant & Casseday 1986, Spangler et al. 1985). Thus, LSO neurons are referred to as IE, or inhibited by contralateral and excited by ipsilateral sound. This property confers sensitivity to ILDs: The firing rate of LSO neurons increases as the sound location changes from contralateral to ipsilateral space.

The LSO is biased towards higher frequencies than the MSO (Gómez-Álvarez & Saldaña 2016, Guinan et al. 1972, Tsuchitani & Boudreau 1966). The combination of a difference in frequency bias (i.e., low in MSO, high in LSO) and a difference in binaural sensitivity (to ITDs in the MSO and to ILDs in the LSO) has led to the classical duplex view of these two binaural nuclei, which appears in most textbooks. It makes a tidy story indeed that these two brainstem circuits are dedicated to the extraction of the two binaural cues; however, this is a mischaracterization, particularly for the LSO.

6. MONAURAL PREPROCESSING

The coding of stimulus fine structure is a hallmark property of the auditory system and is taken to an extreme in bushy-type neurons. These feature large conductances with fast kinetics, low input resistance, and a short time constant, properties geared toward temporal coding (reviewed in Young & Oertel 2004). Sound-evoked responses of bushy-type neurons share general features with AN fibers, hence the term primary-like. However, axonal recordings reveal strongly enhanced phase locking to low-frequency tones compared to the AN (Joris et al. 1994a,b) in two ways. First, spikes occur over a narrower fraction of the stimulus cycle. The resulting peakedness of the cycle histograms (**Figure 6*a***) is quantified by the vector strength (Goldberg & Brown 1969), a number between zero (no preferred phase) and unity (all spikes in a single bin). In the AN, pure-tone vector strength rarely exceeds 0.9, but in high-sync bushy cells, values near 1 occur for frequencies up to almost 1 kHz. Second, bushy-type cells are also more consistent in firing a spike on every cycle. Such entrainment results in strikingly unimodal interspike interval histograms. AN fibers do not entrain; they tend to skip cycles and generate multimodal histograms. These two aspects, accurate temporal coding and superior entrainment, are also obvious in responses to nonperiodic sounds such as wideband noise (**Figure 6*b***), but they can no longer be quantified in terms of vector strength and the fraction of skipped cycles because those metrics require strict periodicity.

Shuffled autocorrelograms (SACs) (Joris 2003) provide an analysis that does not require periodic stimuli. The algorithm has a natural resemblance to the cellular process of coincidence detection (see the sidebar titled Coincidence Detection). The stimulus is repeated *n* times, and pairs

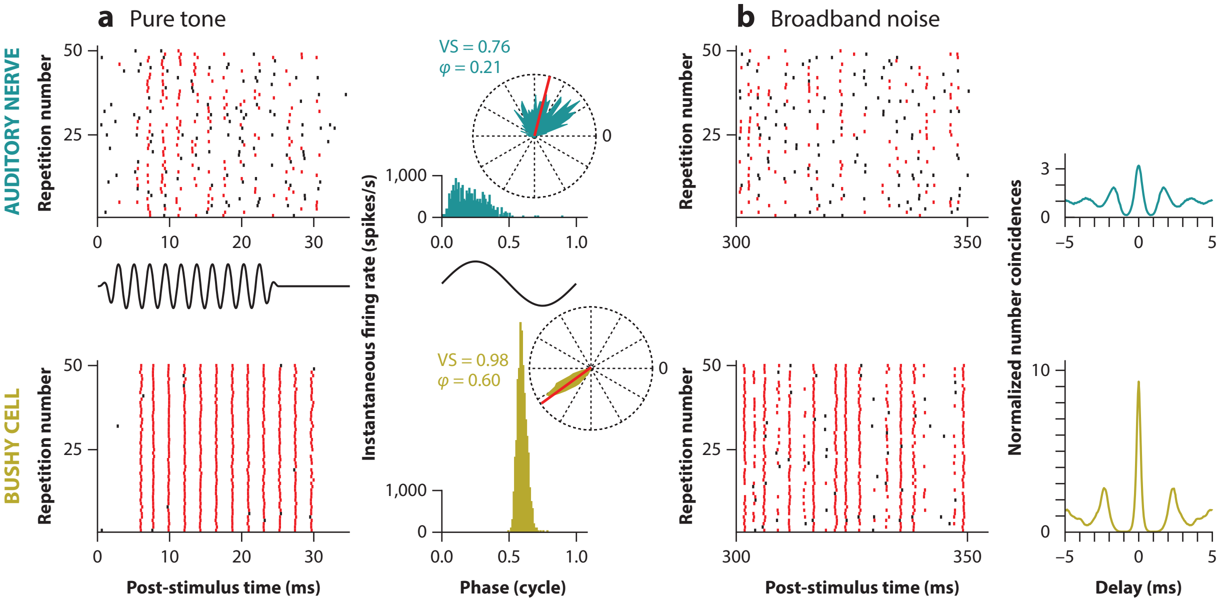

Figure 6

Enhancement of temporal coding from the auditory nerve (AN) to a bushy cell, both tuned near 500 Hz. (*a*) Response to a 460-Hz tone, repeated 50 times. Dot rasters represent the temporal firing pattern; red dots represent spikes occurring at the same instant (within 50 μs) in at least one other stimulus repetition. Phase locking in the AN (*top*) is manifest in the vertical dot alignment and the unimodal cycle histograms. The limited temporal precision of AN firing is reflected by the imperfect dot alignment, the large fraction of unmatched spikes (*black dots*), the shallow-peaked histogram, and the vector strength (VS) of 0.76. The enhanced temporal coding by bushy cells (*lower panels*) is evident from the near-perfect dot alignment, complete dominance of matched spikes (*red dots*), sharply peaked histogram, and VS of 0.98 (**Supplemental Video 1**). (*b*) Responses to wideband noise. Responses show the same enhancement of temporal precision, again reflected by the improved alignment and dominance of matched spikes. Cycle histograms and VS cannot be defined for a noise stimulus, but normalized shuffled autocorrelograms (SACs) provide a quantitative analysis of temporal precision. The SAC of the bushy-cell response (*bottom*) has a much narrower and higher central peak than the SAC of the AN response (*top*). Figure adapted from Joris et al. (2006a).

COINCIDENCE DETECTION

An increase in output spikes following an increase in input spikes is a generic property of neurons; so why do neurons of the medial superior olive (MSO) qualify as coincidence detectors? In a binaural context, the term coincidence detection subsumes several aspects. First, MSO neurons act as multipliers: They tend to fire only when both ears give input spikes at the same instant in time. If input spike trains are conceived of as series of zeros and ones, the output approaches a point-by-point multiplication of the inputs (cf. AND gate) rather than a summation (cf. OR gate). However, the distinction between multiplication and summation is graded rather than dichotomous. For example, MSO neurons typically also respond to monaural stimuli, albeit at a low firing rate. A second aspect of coincidence detection is its timescale, which is extraordinarily short in MSO neurons: Events are coincident when they occur within a submillisecond temporal window. A third aspect that is implicit in the idea that MSO neurons behave as coincidence detectors is that the interaural time delay at which they fire maximally is equal (but opposite in sign) to the time difference at which they receive input spikes from each ear.

of spike trains are evaluated in terms of coincidences, i.e., spikes occurring at the same instant in post-stimulus time. For example, **Figure 6** indicates matched spikes, spikes for which at least one coincident spike occurred in another stimulus repetition. The coincidence count is much higher for the bushy cell than for the AN fiber. Repeating the count with a time shift δ introduced between each pair of spike trains being compared, and varying δ, yields the full correlogram (**Figure 6*b***, right column). For the neurons in **Figure 6** (CF ~ 500 Hz), a 1-ms delay produces a very low coincidence count, whereas a 2-ms delay (close to the characteristic period, CF^{-1}) produces a peak.

Correlogram: histogram summarizing the temporal relationship between events; a discrete version of the correlation function

Correlograms provide a bridge between monaural temporal properties and binaural sensitivity. Consider a perfect coincidence detector receiving two identical bushy cell inputs. If a wideband noise with variable ITD is presented to the two ears, the correlogram describes the ITD function (i.e., the variation of firing rate with ITD) of this idealized detector. And if the two inputs reach the detector with a latency difference (e.g., due to differences in path length), its output is a horizontally shifted version of the correlogram, now peaking at a nonzero BD. Alternatively, δ can be seen as the internal delay: The correlogram then describes the activation pattern of a population of coincidence detectors in response to noise with the ITD equal to zero, each receiving the same input but with different internal delay.

The enhanced temporal coding between AN and bushy-type neurons is interesting in itself. Models of this transformation (reviewed in Joris & Smith 2008) use a monaural form of coincidence detection. Bushy-type neurons code the stimulus more precisely and reliably (**Figure 6**), and this should benefit interaural temporal comparisons. Another less obvious benefit is the robustness against intensity variations: If exactly one spike is fired for each cycle, the firing rate is clamped at the stimulus frequency and therefore insensitive to suprathreshold changes in stimulus intensity. This likely contributes to the striking invariance in firing rates that binaural neurons can display with changes in stimulus intensity (Yin et al. 1986) and may help solve the so-called Steven's problem (van de Par et al. 2001) and Steve's problem (Colburn & Isabelle 2001), which address the difficulty of binaural cross-correlation models to deal with stimulus-level variability.

Several studies have used the correlogram technique to analyze whether enhanced temporal coding by bushy-type neurons improves binaural sensitivity. Simulated ITD sensitivity to fine structure and envelope was indeed much higher when based on spike trains from bushy-type neurons than from AN fibers (van der Heijden et al. 2011). Likewise, neural thresholds for correlation discrimination were better when bushy cells were used for coincidence detection rather than nerve fibers and could be as low as observed in humans (Louage et al. 2006). That study also addresses the potential advantage of having a population of coincidence detectors with different internal delays spanning the range observed in binaural neurons. Access to large internal delays was found to be beneficial for correlation discrimination of narrowband signals, for which the ITD function shows large secondary peaks. Such secondary peaks are less prominent in response to wideband noise. This may explain the psychophysical paradox that decorrelation detection at low frequencies is better for narrowband than for broadband low-frequency noise (Gabriel & Colburn 1981).

7. OUTPUT OF THE SUPERIOR OLIVARY COMPLEX

7.1. Forms of Interaural Time Difference Sensitivity to Ongoing Sound

The first demonstration of ITD sensitivity at the single-cell level was in the inferior colliculus (IC) (Rose et al. 1966). **Figure 7*a*,*b*** illustrates ITD tuning in two IC neurons in response to a broadband noise. ITD is varied over a range much larger than the headwidth. Positive ITDs refer to a stimulus leading in the contralateral ear. The black line in **Figure 7*a*** is representative of most responses recorded in the IC and shows the strong dependence of firing rate on ITD in the shape of a damped oscillation. A central peak at the BD is flanked by deep troughs and smaller

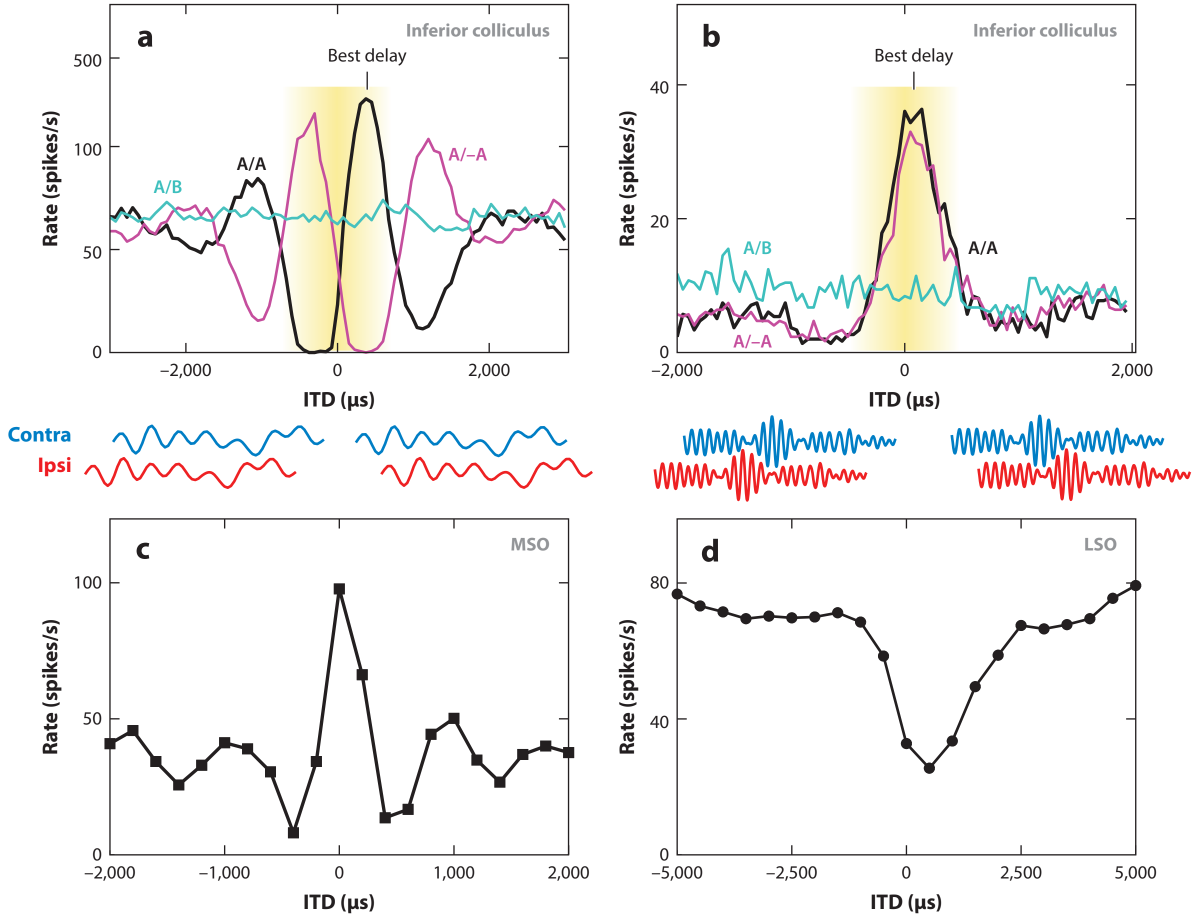

Figure 7

Sensitivity to interaural time delays (ITDs) of a noise stimulus in the (*a*,*b*) inferior colliculus, (*c*) medial superior olive (MSO), and (*d*) lateral superior olive (LSO). Panels *a* and *c* show low-frequency neurons, (*a*) 405 Hz and (*c*) 780 Hz, and panels *b* and *d* show high-frequency neurons, (*b*) 5,220 Hz and (*d*) 5,040 Hz. Black lines are responses to ITDs of identical (correlated) noise in the two ears (A/A); the magenta line indicates the response to anticorrelated noise (A/−A); and the cyan line shows the response to uncorrelated noise (A/B). The yellow rectangle shows the approximate headwidth. The waveforms between the upper and lower panels are diagrams, for a positive and negative ITD, of vibration at the cochlear place from which the neuron ultimately derives its input. Neurons were recorded in cat (*a*,*b*,*d*) and gerbil (*c*). Panels *a* and *b* adapted from Joris (2003), panel *c* adapted from Plauška et al. (2017), and panel *d* adapted from Joris & Yin (1995).

secondary peaks. If the two ears are stimulated by independently generated noise waveforms, noise A in one ear and B in the other ear (A/B) (**Figure 7*a*,*b***), there is no systematic ongoing ITD but only a varying gating or onset ITD (cf. **Figure 3*c***), which has no effect on overall spike rate. In the condition with A/−A, the noise token is identical at the two ears, but the polarity of the noise is inverted at one ear (as if reversing the two earphone wires). The resulting response is antiphasic relative to the response to correlated noise. This is to be expected: Waveform inversion corresponds to a π phase shift of all stimulus components. Interestingly, very similar response patterns to correlated and anticorrelated random-dot patterns are observed in disparity-selective neurons in primary visual cortex (Cumming & Parker 1997).

THE ACOUSTIC CHIASM

Projections of the medial superior olive (MSO) and lateral superior olive (LSO) form the acoustic chiasm (Masterton & Imig 1984). While the MSO gives excitatory projections to the ipsilateral inferior colliculus (IC), the LSO makes excitatory projections to the contralateral IC and largely inhibitory projections ipsilaterally (**Figure 5**). From the midbrain upward, neurons are driven by sounds in contralateral space, and lesions result in localization deficits in contralateral space (Champoux et al. 2007, Jenkins & Masterton 1982, Litovsky et al. 2002).

The response in **Figure 7*b*** shows another form of ITD sensitivity. Again, the BD is positive, but the ITD function shows a single peak surrounded by shallow troughs. Moreover, the ITD function obtained from anticorrelated noise is virtually identical. This type of sensitivity is observed less frequently [and is little documented at the level of the MSO (Joris 1996, Plauška et al. 2016, Yin & Chan 1990)], but it is the dominant kind of response observed at higher (>2 kHz) CFs (Devore & Delgutte 2010, Joris 2003). It indicates that the neuron is sensitive to ITDs of the envelope rather than the fine structure of the waveform. The envelope is symmetric and therefore not affected by changing the polarity in one ear. The use of independent noises removes correlation in both fine structure and envelope and again results in a low response rate independent of the ITD (**Figure 7*b***). There is also a minority of IC responses (troughers) better described as being tuned in an inhibitory direction (Batra et al. 1997, McAlpine et al. 2001, Yin et al. 1986).

7.2. Distribution of Best Delays

A consistent finding in the IC is that BDs are mostly positive, i.e., neurons are most active when the contralateral stimulus precedes the ipsilateral one. Studies in cat (Hancock & Delgutte 2004, Yin et al. 1986) found that the range of BDs covers the headwidth of these animals [about 350 to 400 μs (Roth et al. 1980)]. These findings nicely fit the general notion of a tuned system that covers the perceptually relevant cue range and that is contralateralized like the visual and somatosensory systems (see the sidebar titled The Acoustic Chiasm). This notion was challenged by the discovery that the range of BDs is CF dependent: The upper bound is roughly hyperbolic at a constant phase value of π, the so-called π-limit. This was first described in guinea pig (McAlpine et al. 1996, 2001), and similar distributions have been found in IC and MSO recordings of various species, including cat (Hancock & Delgutte 2004, Joris et al. 2006b), gerbil (Brand et al. 2002, Day & Semple 2011, Pecka et al. 2008, Plauška et al. 2017), and chinchilla (Bremen & Joris 2013). This finding has implications for the mechanism underlying the BD, but the functional implications are less clear.

According to the two-channel model (McAlpine et al. 2001), the observed scattering of BDs is a bug rather than a feature; ITD tuning is not optimized to have a range of BDs spanning the headwidth at all frequencies, but rather to have the steepest slope of sensitivity centered at zero ITD (Harper & McAlpine 2004). It is proposed that binaural temporal sensitivity relies on a comparison of two channels that show a sigmoidal dependence of firing rate for ITDs within the headwidth, a push-pull system in which two populations of MSO neurons, one in each hemisphere, respond in opposite directions to a given stimulus.

Although the two-channel model may be adequate for the lateralization of simple stimuli such as single tones, its plausibility beyond such stimuli has been questioned by computational studies (Brette 2010, Day et al. 2012, Fitzpatrick et al. 1997, Goodman et al. 2013, Hancock 2007, van der Heijden et al. 2011). Furthermore, the argument for optimal slope positioning ignores the fact that neural sensitivity to decorrelation is largest at the peaks of ITD sensitivity, not at the slopes (Coffey et al. 2006, Joris et al. 2006c, Louage et al. 2006, Shackleton et al. 2005, Yin et al. 1987). This can be observed in **Figure 7*a***: ITD functions for the three conditions of correlation have their largest differences near the BD. Also, unilateral lesions at the level of the midbrain or higher impair sound localization in contralateral but not ipsilateral space (see the sidebar titled The Acoustic Chiasm). These and other observations make the two-channel model untenable.

8. MECHANISMS OF SENSITIVITY TO INTERAURAL TIME DIFFERENCE

There are vastly more data from the midbrain than from the SOC, from which the IC inherits its ITD sensitivity. Prominent phase-locked, local field potentials (Mc Laughlin et al. 2010), small action potentials (L.L. Scott et al. 2007), and small target size combined with poor accessibility make single-cell recording in the SOC challenging. The positive identification of physiologically characterized principal MSO and LSO neurons was recently achieved by intracellular labeling (Franken et al. 2015, 2018), but it is not entirely clear whether the MSO and LSO are the only primary sources of ITD sensitivity, which has often been observed in other SOC locations (Batra et al. 1997, Day & Semple 2011, Franken et al. 2016a, Goldberg & Brown 1969).

Examples of ITD sensitivity to noise of an MSO and LSO neuron are shown in **Figure 7*c*,*d***. Nearly all published MSO responses are dominated by fine structure, whereas most LSO responses are dominated by envelope. Note that the ITD function of the LSO neuron is of the trougher variety, as expected from its IE binaural interaction: When ipsi- and contralateral inputs to the cell are maximally correlated, the cell is maximally inhibited.

Two concepts that have taken center stage in SOC studies of ITD sensitivity are internal delays and coincidence detection. We first discuss these concepts for the MSO and conclude with LSO physiology.

8.1. Internal Delay

The mechanism(s) behind the range of BDs surmised psychophysically and observed physiologically sparked much debate. Much of this debate centers on the sources and respective roles of time and phase delays in the origin of the BD and is reminiscent of a similar debate in vision regarding position and phase mechanisms in disparity selectivity (Cumming & DeAngelis 2001). **Figure 8*a*** illustrates internal delay, the difference in delay between the effective input of the left versus right ear on the binaural neuron. If the stimulus ITD is compensated for by internal delay, the effective inputs are coincident and the neuron is optimally excited. The finding of an inverse relationship between internal delay (estimated by BD) and CF (McAlpine et al. 1996, 2001) suggests a mechanism that somehow scales with CF^{-1}.

Jeffress (1948) proposed that internal delays are produced by axonal delay lines. **Figure 8*b*** shows a rendition based on axonal tracing (Beckius et al. 1999, Smith et al. 1993): Branches of the contralateral SBCs toward the rostral pole of the MSO tend to be shorter than toward its caudal pole. Systematic differences in axonal length between ipsilateral and contralateral inputs would not only create a range of BDs at each frequency but also a rostrocaudal map of BDs. Such a gradient was indeed suggested by MSO recordings (Yin & Chan 1990) in a direction consistent with the axonal tracing data. Thus, both anatomical and physiological data supported Jeffress's proposal (Joris et al. 1998). However, this interpretation is challenged by the finding of the inverse BD-CF relationship (McAlpine et al. 2001), which is not predicted by (although not necessarily inconsistent with) axonal delay lines. A reanalysis confirmed the existence of gradients in axonal length but estimated that the resulting delays were too small, particularly at low CF, and could not account

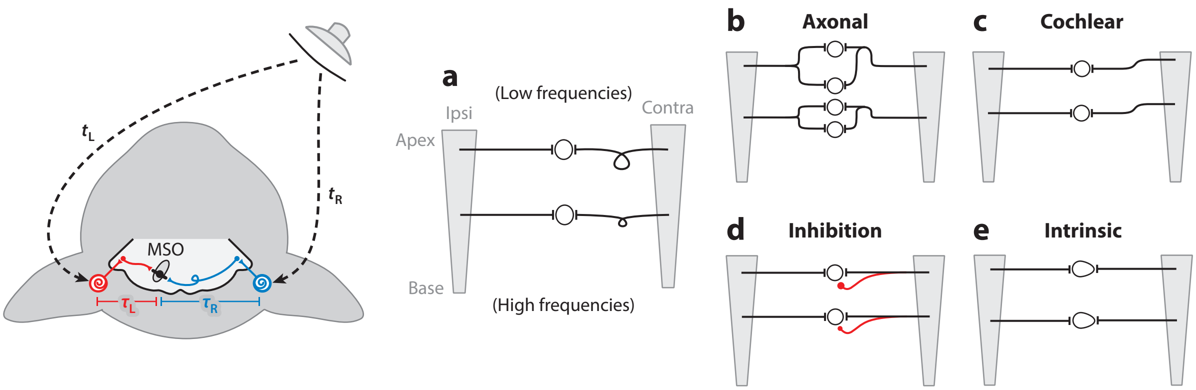

Figure 8

Diagram of hypothesized sources of internal delay. The trapezoidal shapes in each panel represent the basilar membranes of the ipsi- and contralateral ear. Circles are medial superior olive (MSO) neurons with simplified inputs. (*a*) The observed distribution of internal delays shows a longer effective delay contralaterally than ipsilaterally, symbolized by a loop, and a larger difference at lower (*larger loop*) compared to higher frequencies (*shorter loop*). (*b*) Jeffress (1948) proposed axonal delay lines creating a range of internal delays at all frequencies. The delay lines would need to be longer at the lowest frequencies. (*c*) Schroeder (1977) proposed an asymmetry in cochlear innervation causing a lower characteristic frequency (more apical location) of contralateral than ipsilateral inputs. (*d*) Brand et al. (2002) proposed delay of the contralateral input by preceding inhibition (*red*). (*e*) Some sources of delay are proposed to be intrinsic to the nucleus.

for the BD distribution in cat (Karino et al. 2011). Perhaps gradients in axonal diameter or internodal distance are important variables (Ford et al. 2015, Seidl et al. 2010). However, the labeling of physiologically characterized MSO neurons in gerbil did not support a rostrocaudal map of BDs (Franken et al. 2015). Furthermore, axonal delays are pure time delays, whereas ITD functions often express a constant phase delay between the inputs from the two ears [MSO (Plauška et al. 2016), IC (Yin & Kuwada 1983)]. This produces asymmetric ITD functions (**Figure 7*a***) in which the secondary peak on one side of the main peak is smaller than on the other side (unlike the SACs in **Figure 6*b***). These asymmetries provide further evidence of mechanisms other than pure time delays. Thus, at present, the central tenet of Jeffress's model, axonal delay lines producing a map of ITDs, no longer appears plausible.

The systematic delays created by the cochlear traveling wave motivated another proposal for internal delay (Schroeder 1977). If the inputs from the two ears are mismatched in CF, the input from the ear with lower CF incurs a delay (**Figure 8*c***). Computational models and a correlation analysis of AN spike trains tested the plausibility of this scheme (Bonham & Lewis 1999, Joris et al. 2006b, Shamma et al. 1989). Small cochlear disparities are sufficient to generate delays that are significant in binaural terms, and interestingly they scale with CF^{-1} (Joris et al. 2006b) and can account for other features of ITD sensitivity (Benichoux et al. 2015). A difficulty with this proposal is that while an error in wiring seems plausible, it should be systematic; a bias of contralateral inputs toward a lower CF than ipsilateral inputs is needed to generate positive BDs. An examination in gerbil found evidence for a cochlear contribution to BD but no correlation between mismatches in frequency tuning and BD (Plauška et al. 2017). Binaural reverse correlation analysis of MSO neurons also revealed tuning mismatches, which, moreover, were biased toward the contralateral ear (Sayles et al. 2016). Thus, although there is suggestive evidence that cochlear disparities contribute to BD (see also Benichoux et al. 2015, Day & Semple 2011), the weight of that contribution is unclear.

Inhibition was proposed as a source of internal delay (Batra et al. 1997, Brand et al. 2002): Contralateral inhibition would delay contralateral excitation (**Figure 8*d***), which would generate a within-cycle phase shift rather than a time delay. Modeling (Day & Semple 2011, Zhou et al. 2005) and in vitro physiology (Myoga et al. 2014, Roberts et al. 2014) showed that the effects are too small to explain the range of BDs observed, and in vivo juxtacellular and whole-cell recordings do not support an effect of leading inhibition (Franken et al. 2015, van der Heijden et al. 2013). Also, inhibitory terminals are heavily concentrated on MSO somata (Kapfer et al. 2002) so that any delaying or advancing effects would affect both ipsilateral and contralateral inputs.

A recent study (van der Heijden 2018) proposes that interaural asymmetries in the activation threshold of inner hair cell synapses may contribute to internal delays. This hypothesis has not yet been tested experimentally.

There have been several suggestions for sources of delay intrinsic to MSO neurons (**Figure 8*e***). Their axon can have a dendritic rather than somatic origin (Smith 1995), which could introduce a differential delay (Zhou et al. 2005). However, this structural asymmetry is only present in a minority of cells (Rautenberg et al. 2009), and the predicted asymmetry in excitatory postsynaptic potential (EPSP)–action potential latency was not observed in vivo (van der Heijden et al. 2013). An asymmetry in the rise time of contralaterally versus ipsilaterally evoked EPSPs was proposed to introduce a differential delay (Jercog et al. 2010), but the asymmetry was not replicated in vitro (Roberts et al. 2014) and in vivo (Franken et al. 2015, van der Heijden et al. 2013). Franken et al. (2015) found that asymmetries in the temporal pattern of ipsilateral and contralateral excitation interacted with membrane properties to generate phase delays. These asymmetries were correlated with CF, but their sources have not been established.

BDs amount to only a fraction of the overall latency between sound stimulus and MSO response (~4 ms). It is interesting that the diverse mechanisms examined give rather underwhelming delays. This easily leads to floccinaucinihilipilification of the respective mechanisms, but it is at once an indication of the optimization in this circuit to tightly control timing. There is the unalluring but real possibility that a combination of factors is at work, perhaps to different degrees in different neurons. Possibly the circuit is tweaked, phylogenetically and/or ontogenetically, to limit BDs to a behaviorally relevant range without there being one specific and dominant mechanism for internal delay.

8.2. Coincidence Detection in the Medial Superior Olive

Coincidence detection was an early concept in models implying neural multiplication (referred to as summation in Jeffress 1948, Licklider 1951, McCulloch & Pitts 1943). Mechanistically, it entails several subcomponents (see the sidebar titled Coincidence Detection). Initial tests of coincidence detection focused on the relationship between BD and the timing of monaural responses by comparing spike output to monaural and binaural stimulation. Goldberg & Brown (1969) showed that the difference in phase of monaural responses to tones matched the ITD of maximal binaural response. Yin & Chan (1990) extended this analysis to amplitude-modulated tones and noise. However, comparison of the output of the same neuron to monaural and binaural stimulation is not the same as comparing input and output. Such analysis became possible with methods enabling the recording of both subthreshold and spike events (Franken et al. 2015, van der Heijden et al. 2013). **Figure 9** shows an in vivo, whole-cell MSO recording. Ipsilateral and contralateral monaural stimulation give rise to brief, spike-like, subthreshold EPSPs that are phase-locked to the tonal stimulus, sometimes triggering small action potentials. With the stimuli combined into a binaural beat, the in-phase part of the stimulus evokes large and well-phase-locked EPSPs, which trigger spikes, and the antiphase part evokes noncoincident EPSPs, which remain subthreshold.

There has been much in vitro work to understand the cellular mechanisms enabling coincidence detection (see the sidebar titled Cellular Specializations), but its exact form in vivo is

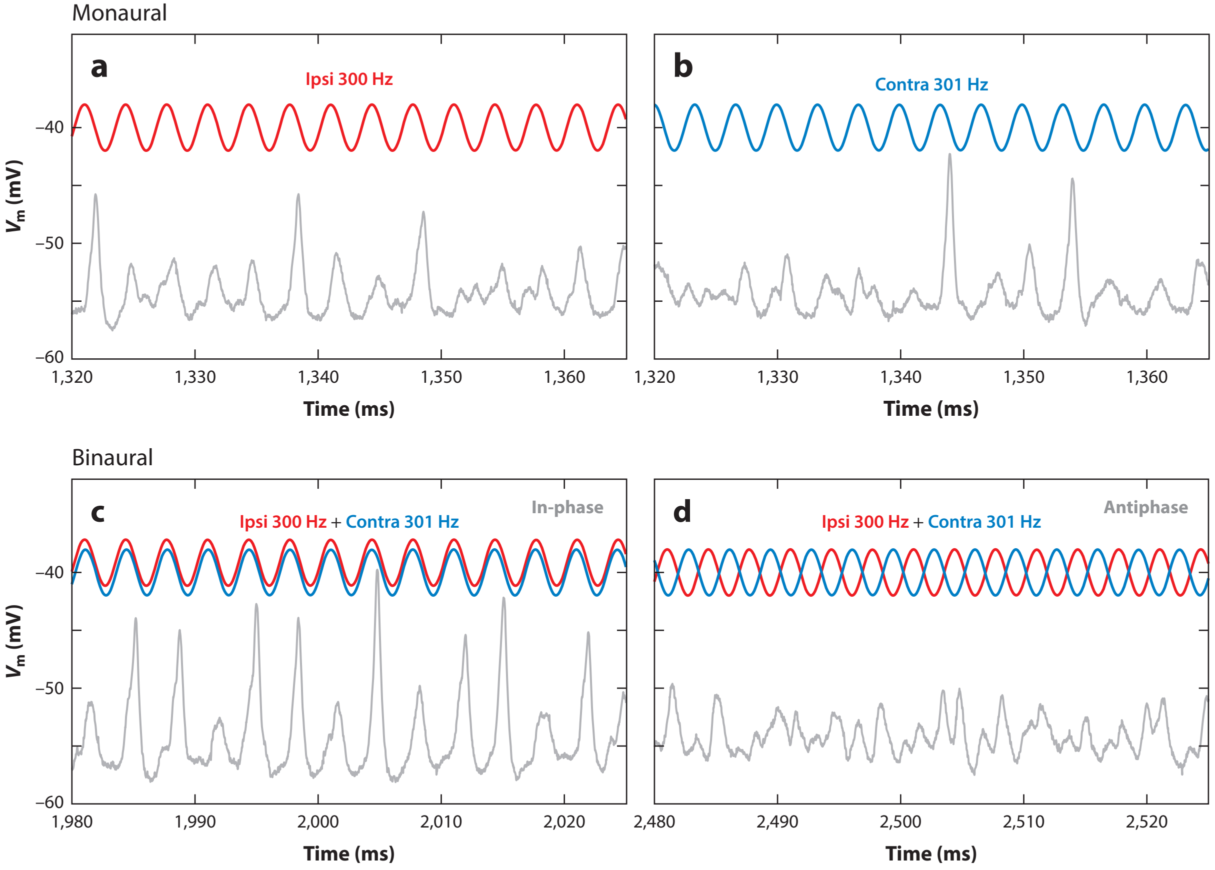

Figure 9

Example traces of a gerbil medial superior olive neuron in response to tones (300 and 301 Hz) with a 1-Hz binaural beat. Each response shows a 45-ms snippet from a 5-s-long recording to tones presented (*a*,*b*) monaurally or (*c*,*d*) binaurally. With monaural stimulation, small action potentials, variable in amplitude, are present at low rates. When presented together, the phase of the tones drifts alternatingly (*c*) in-phase and (*d*) antiphase, and activity varies between (*c*) high rates and (*d*) no spiking (**Supplemental Video 2**). Data provided by T.P. Franken.

CELLULAR SPECIALIZATIONS

Recent in vitro studies (reviewed in Golding & Oertel 2012) uncovered the extraordinary cellular specializations underlying coincidence detection at the timescale needed in the medial superior olive. Models drew attention to the need for a mechanism to reduce monaural autocoincidences (Colburn et al. 1990, Franken et al. 2014): This is thought to be a dendritic function tied to the segregation of ipsi- and contralateral afferents to opposite dendrites (Agmon-Snir et al. 1998, Golding & Oertel 2012). EPSPs are shaped by a low-voltage-activated K^+ conductance to maintain a short time course while propagating from dendrites to soma. Large resting conductances (g_{KL} and g_h) make the cells leaky and decrease the membrane time constant. The neurons are electrically compartmentalized so that action potentials show poor backpropagation from the axon to the soma, which contributes to the difficulties in extracellular recordings of spikes.

disputed. Juxtacellular in vivo recordings of gerbil MSO showed that a simple linear summation of subthreshold events combined with a threshold nonlinearity predicted spike output to tones (van der Heijden et al. 2013) and broadband stimuli (Plauška et al. 2016). However, whole-cell recordings in the same species revealed discrepancies between the timing of EPSPs and BDs (Franken et al. 2015). These were traced to subtle asymmetries in the pattern of activation to ipsilateral and contralateral inputs, which, in interaction with the cell's membrane properties, cause ordering effects that generate a phase shift in ITD sensitivity. The latter finding suggests a coupling between the process of internal delay and coincidence detection.

9. THE LATERAL SUPERIOR OLIVE AS A COMPLEMENTARY INTERAURAL TIME DIFFERENCE PROCESSOR

Neuroscience textbooks invariably refer to the LSO as the ILD processor. While MSO neurons perform a multiplication-type operation, LSO neurons are typically characterized as subtractors (reviewed in Tollin 2003). Because the two ears have opposite synaptic effects, the firing of LSO neurons indeed signals whether sound intensity is larger at the ipsilateral (high firing rate) or contralateral ear (no firing). There are several reasons to suspect that such characterization of the LSO is incomplete (reviewed in Joris & Trussell 2018). The assumption that the LSO only processes ILDs is difficult to square with many specializations of this circuit (**Figure 5*b***) that suggest a role in timing, such as the calyx of Held (see the sidebar titled Giant Synapses). As discussed above, behavioral ITD sensitivity extends to high frequencies based on the stimulus envelope (cf. **Figure 7*b***), so the processing of envelope ITDs may seem to be a plausible raison d'être of the temporal specializations. Indeed, LSO neurons show ITD sensitivity to amplitude-modulated, high-frequency sounds and even some sensitivity to ITDs of fine structure at low frequencies (Finlayson & Caspary 1991; Joris & Yin 1995; Tollin & Yin 2002, 2005); however, in both cases, ITD sensitivity is rather weak and easily swamped by ILDs, which seems incommensurate with the extraordinary specializations such as the calyx. The only case in which LSO neurons show a steep ITD dependence over a range of ILDs is to stimulus transients such as clicks (Irvine et al. 2001, Joris & Yin 1995). Recent data (Franken et al. 2016b) confirm steep ITD sensitivity to clicks in LSO but not MSO neurons. Transients may thus be the only temporal stimulus feature for which ITD sensitivity is superior in the LSO compared to MSO. Joris & Trussell (2018) proposed that the behavioral relevance of this sensitivity is in the spatial lateralization of transients produced adventitiously during animal locomotion (rustling sounds).

Recent data (Franken et al. 2018) add a surprising twist. The LSO is less homogenous than the MSO; besides principal cells, which constitute the bulk of the nucleus, other morphological classes are distinguished (Helfert & Schwartz 1986). By labeling physiologically characterized cells, Franken et al. (2018) found that principal cells do not generate the classical sustained (i.e., chopper) pattern of response, associated with the LSO since the earliest single-unit studies (Boudreau & Tsuchitani 1968, Guinan et al. 1972). Rather, principal cells are MSO-like, with similar membrane features (i.e., short time constants, short post-synaptic potentials, small action potentials). These cells generate onset responses to pure tones and appear to be the neurons with acute ITD sensitivity to transients. Franken et al. (2018) suggested that traditional extracellular recording methods, used in previous studies, biased against recording from principal cells.

10. SUMMARY AND OUTLOOK

Great strides have been made in the past two decades in the study of the initial temporal binaural interactions in the brainstem. Various new techniques, both in vivo and in vitro, have yielded much refined knowledge of these reticent nuclei, and there is a healthy variety of hypotheses and models to drive further experimentation. In the near future, technical advances will further refine morphological resolution of the circuit and allow for its optical manipulation towards both mechanistic and functional questions. Little is known regarding binaural response features that are not simply inherited from the SOC but arise at higher anatomical levels. Also, the effort toward understanding mechanisms underlying ITD sensitivity to simple, single sources has detracted from more functional themes of inquiry. How do binaural responses help to solve real-world problems such as separating sound sources, dealing with reflections, estimating distance, and detecting weak signals? Studies at the midbrain and thalamocortical levels are needed to understand how the output of the brainstem binaural nuclei is read out and integrated with monaural spatial and nonspatial cues. Increasing our knowledge of this system is not just of academic interest: Deficient ITD sensitivity is a key problem in the hearing-impaired for reasons that are only partly understood (Chung et al. 2016).

DISCLOSURE STATEMENT

The authors are not aware of any affiliations, memberships, funding, or financial holdings that might be perceived as affecting the objectivity of this review.

ACKNOWLEDGMENTS

We thank Natalie and Christa for their award-winning hospitality during the preparation of this review. Our research is currently supported by the Research Foundation–Flanders (G0B2917N), the Bijzonder Onderzoeksfonds KU Leuven (OT-14-118) (P.X.J.), and the Netherlands Organization for Scientific Research (ALW 824.15.008) (M.v.d.H.). We dedicate this review to our contra- and ipsilateral inputs, Tom Yin and Tino Trahiotis.

LITERATURE CITED

Agmon-Snir H, Carr CE, Rinzel J. 1998. The role of dendrites in auditory coincidence detection. *Nature* 393:268–72

Banks MI, Smith PH. 1992. Intracellular recordings from neurobiotin-labeled cells in brain slices of the rat medial nucleus of the trapezoid body. *J. Neurosci.* 12:2819–37

Batra R, Kuwada S, Fitzpatrick DC. 1997. Sensitivity to interaural temporal disparities of low- and high-frequency neurons in the superior olivary complex. I. Heterogeneity of responses. *J. Neurophysiol.* 78:1222–36

Beckius GE, Batra R, Oliver DL. 1999. Axons from anteroventral cochlear nucleus that terminate in medial superior olive of cat: observations related to delay lines. *J. Neurosci.* 19(8):3146–61

Benichoux V, Fontaine B, Franken TP, Karino S, Joris PX, Brette R. 2015. Neural tuning matches frequency-dependent time differences between the ears. *eLife* 4:e06072

Bernstein LR. 2001. Auditory processing of interaural timing information: new insights. *J. Neurosci. Res.* 66(6):1035–46

Bernstein LR, Trahiotis C. 2018. Effects of interaural delay, center frequency, and no more than "slight" hearing loss on precision of binaural processing: empirical data and quantitative modeling. *J. Acoust. Soc. Am.* 144(1):292

Blodgett HC, Wilbanks WA, Jeffress LA. 1956. Effect of large interaural time differences upon the judgment of sidedness. *J. Acoust. Soc. Am.* 28(4):639–43

Bonham BH, Lewis ER. 1999. Localization by interaural time difference (ITD): effects of interaural frequency mismatch. *J. Acoust. Soc. Am.* 106:281–90

Boudreau JC, Tsuchitani C. 1968. Binaural interaction in the cat superior olive S segment. *J. Neurophysiol.* 31:442–54

Brand A, Behrend O, Marquardt T, McAlpine D, Grothe B. 2002. Precise inhibition is essential for microsecond interaural time difference coding. *Nature* 417:543–47

Bremen P, Joris PX. 2013. Axonal recordings from medial superior olive neurons obtained from the lateral lemniscus of the chinchilla (*Chinchilla laniger*). *J. Neurosci.* 33(44):17506–18

Brette R. 2010. On the interpretation of sensitivity analyses of neural responses. *J. Acoust. Soc. Am.* 128(5):2965–72

Brown C, May BJ. 2005. Comparative mammalian sound localization. In *Sound Source Localization*, ed. A Popper, R Fay, pp. 124–78. New York: Springer

Cant NB. 1984. The fine structure of the lateral superior olivary nucleus of the cat. *J. Comp. Neurol.* 227:63–77

Cant NB, Casseday JH. 1986. Projections from the anteroventral cochlear nucleus to the lateral and medial superior olivary nuclei. *J. Comp. Neurol.* 247(4):457–76

Cant NB, Hyson RL. 1992. Projections from the lateral nucleus of the trapezoid body to the medial superior olivary nucleus in the gerbil. *Hear. Res.* 58:26–34

Champoux F, Paiement P, Mercier C, Lepore F, Lassonde M, Gagné J-P. 2007. Auditory processing in a patient with a unilateral lesion of the inferior colliculus. *Eur. J. Neurosci.* 25(1):291–97

Chung Y, Hancock KE, Delgutte B. 2016. Neural coding of interaural time differences with bilateral cochlear implants in unanesthetized rabbits. *J. Neurosci.* 36(20):5520–31

Clark GM. 1969. Vesicle shape versus type of synapse in the nerve endings of the cat medial superior olive. *Brain Res.* 15(2):548–51

Coffey CS, Ebert CS Jr., Marshall AF, Skaggs JD, Falk SE, et al. 2006. Detection of interaural correlation by neurons in the superior olivary complex, inferior colliculus and auditory cortex of the unanesthetized rabbit. *Hear. Res.* 221(1–2):1–16

Colburn HS, Durlach NI. 1978. Models of binaural interaction. In *Hearing*, ed. EC Carterette, MP Friedman, pp. 467–518. New York: Academic

Colburn HS, Han YA, Cullota CP. 1990. Coincidence model of MSO responses. *Hear. Res.* 49:335–46

Colburn HS, Isabelle SK. 2001. Physiologically based models of binaural detection. In *Physiological and Psychophysical Bases of Auditory Function*, ed. DJ Breebaart, pp. 142–48. Maastricht, Neth.: Shaker Publ. BV

Cumming BG, DeAngelis GC. 2001. The physiology of stereopsis. *Annu. Rev. Neurosci.* 24:203–38

Cumming BG, Parker AJ. 1997. Responses of primary visual cortical neurons to binocular disparity without depth perception. *Nature* 389(6648):280–83

Day ML, Koka K, Delgutte B. 2012. Neural encoding of sound source location in the presence of a concurrent, spatially separated source. *J. Neurophysiol.* 108(9):2612–28

Day ML, Semple MN. 2011. Frequency-dependent interaural delays in the medial superior olive: implications for interaural cochlear delays. *J. Neurophysiol.* 106(4):1985–99

Devore S, Delgutte B. 2010. Effects of reverberation on the directional sensitivity of auditory neurons across the tonotopic axis: influences of interaural time and level differences. *J. Neurosci.* 30(23):7826–37

Durlach NI. 1972. Binaural signal detection: equalization and cancellation theory. In *Foundations of Modern Auditory Theory*, Vol. 2, ed. JV Tobias, pp. 371–462. New York: Academic

Durlach NI, Colburn HS. 1978. Binaural phenomena. In *Hearing*, ed. EC Carterette, MP Friedman, pp. 365–465. New York: Academic

Finlayson PG, Caspary DM. 1991. Low-frequency neurons in the lateral superior olive exhibit phase-sensitive binaural inhibition. *J. Neurophysiol.* 65:598–605

Fitzpatrick DC, Batra R, Stanford TR, Kuwada S. 1997. A neuronal population code for sound localization. *Nature* 388:871–74

Ford MC, Alexandrova O, Cossell L, Stange-Marten A, Sinclair J, et al. 2015. Tuning of Ranvier node and internode properties in myelinated axons to adjust action potential timing. *Nat. Commun.* 6:8073

Franken TP, Bremen P, Joris PX. 2014. Coincidence detection in the medial superior olive: mechanistic implications of an analysis of input spiking patterns. *Front. Neural Circuits.* 8:42

Franken TP, Joris PX, Smith PH. 2018. Principal cells of the brainstem's interaural sound level detector are temporal differentiators rather than integrators. *eLife* 7:e33854

Franken TP, Roberts MT, Wei L, Golding NL, Joris PX. 2015. In vivo coincidence detection in mammalian sound localization generates phase delays. *Nat. Neurosci.* 18(3):444–52

Franken TP, Smith PH, Joris PX. 2016a. In vivo whole-cell recordings combined with electron microscopy reveal unexpected morphological and physiological properties in the lateral nucleus of the trapezoid body in the auditory brainstem. *Front. Neural Circuits* 10:69

Franken TP, Smith PH, Joris PX. 2016b. In vivo whole-cell recordings of the lateral and medial superior olive to interaural time differences of transients. *Assoc. Res. Otolaryngol. Abs.* 39:451

Gabriel KG, Colburn HS. 1981. Interaural correlation discrimination: I. Bandwidth and level dependence. *J. Acoust. Soc. Am.* 69:1394–401

Goldberg JM, Brown PB. 1969. Response of binaural neurons of dog superior olivary complex to dichotic tonal stimuli: some physiological mechanisms of sound localization. *J. Neurophysiol.* 22:613–36

Golding NL, Oertel D. 2012. Synaptic integration in dendrites: exceptional need for speed. *J. Physiol.* 590(22):5563–69

Gómez-Álvarez M, Saldaña E. 2016. Different tonotopic regions of the lateral superior olive receive a similar combination of afferent inputs. *J. Comp. Neurol.* 524(11):2230–50

Goodman DFM, Benichoux V, Brette R. 2013. Decoding neural responses to temporal cues for sound localization. *eLife* 2:e01312

Guinan JJ, Norris BE, Guinan SS. 1972. Single auditory units in the superior olivary complex. II: Locations of unit categories and tonotopic organization. *Int. J. Neurosci.* 4:147–66

Hancock KE. 2007. A physiologically-based population rate code for interaural time differences (ITDs) predicts bandwidth-dependent lateralization. In *Hearing—From Sensory Processing to Perception*, ed. B Kollmeier, G Klump, V Hohmann, U Langemann, M Mauermann, et al., pp. 389–97. Berlin: Springer-Verlag

Hancock KE, Delgutte B. 2004. A physiologically based model of interaural time difference discrimination. *J. Neurosci.* 24:7110–17

Harper NS, McAlpine D. 2004. Optimal neural population coding of an auditory spatial cue. *Nature* 430(7000):682–86

Harrison JM, Irving R. 1966. Visual and nonvisual auditory systems in mammals. Anatomical evidence indicates two kinds of auditory pathways and suggests two kinds of hearing in mammals. *Science* 154(3750):738–43

Heffner RS, Heffner HE. 1992. Visual factors in sound localization in mammals. *J. Comp. Neurol.* 317(3):219–32

Helfert RH, Schwartz IR. 1986. Morphological evidence for the existence of multiple neuronal classes in the cat lateral superior olivary nucleus. *J. Comp. Neurol.* 244:533–49

Henning GB. 1974. Detectability of interaural delay in high-frequency complex waveforms. *J. Acoust. Soc. Am.* 55:84–90

Henning GB. 1980. Some observations on the lateralization of complex waveforms. *J. Acoust. Soc. Am.* 68:446–54

Hirsh IJ. 1948. Binaural summation and interaural inhibition as a function of the level of masking noise. *Am. J. Psychol.* 61(2):205–13

Houtgast T, Steeneken HJM. 1985. A review of the MTF concept in room acoustics and its use for estimating speech intelligibility in auditoria. *J. Acoust. Soc. Am.* 77(3):1069–77

Irvine DR, Park VN, McCormick L. 2001. Mechanisms underlying the sensitivity of neurons in the lateral superior olive to interaural intensity differences. *J. Neurophysiol.* 86(6):2647–66

Jeffress LA. 1948. A place theory of sound localization. *J. Comp. Physiol. Psychol.* 41:35–39

Jenkins WM, Masterton RB. 1982. Sound localization: effects of unilateral lesions in central auditory system. *J. Neurophysiol.* 47(6):987–1016

Jercog PE, Svirskis G, Kotak VC, Sanes DH, Rinzel J. 2010. Asymmetric excitatory synaptic dynamics underlie interaural time difference processing in the auditory system. *PLOS Biol.* 8(6):e1000406

Johnson DH. 1980. The relationship between spike rate and synchrony in responses of auditory-nerve fibers to single tones. *J. Acoust. Soc. Am.* 68:1115–22

Joris PX. 1996. Envelope coding in the lateral superior olive. II. Characteristic delays and comparison with responses in the medial superior olive. *J. Neurophysiol.* 76(4):2137–56

Joris PX. 2003. Interaural time sensitivity dominated by cochlea-induced envelope patterns. *J. Neurosci.* 23(15):6345–50

Joris PX. 2019. Neural binaural sensitivity at high sound speeds: single cell responses in cat midbrain to fast-changing interaural time differences of broadband sounds. *J. Acoust. Soc. Am.* 145(1):EL45–EL51

Joris PX, Carney LH, Smith PH, Yin TC. 1994a. Enhancement of neural synchronization in the anteroventral cochlear nucleus. I. Responses to tones at the characteristic frequency. *J. Neurophysiol.* 71(3):1022–36

Joris PX, Louage DH, Cardoen L, van der Heijden M. 2006a. Correlation index: a new metric to quantify temporal coding. *Hear. Res.* 216–217:19–30

Joris PX, Smith PH. 2008. The volley theory and the spherical cell puzzle. *Neuroscience* 154(1):65–76

Joris PX, Smith PH, Yin TC. 1994b. Enhancement of neural synchronization in the anteroventral cochlear nucleus. II. Responses in the tuning curve tail. *J. Neurophysiol.* 71(3):1037–51

Joris PX, Smith PH, Yin TC. 1998. Coincidence detection in the auditory system: 50 years after Jeffress. *Neuron* 21(6):1235–38

Joris PX, Trussell LO. 2018. The calyx of Held: a hypothesis on the need for reliable timing in an intensity difference encoder. *Neuron* 100:534–49

Joris PX, van de Sande B, Louage DH, van der Heijden M. 2006b. Binaural and cochlear disparities. *PNAS* 103(34):12917–22

Joris PX, van de Sande B, Recio-Spinoso A, van der Heijden M. 2006c. Auditory midbrain and nerve responses to sinusoidal variations in interaural correlation. *J. Neurosci.* 26(1):279–89

Joris PX, Yin TC. 1995. Envelope coding in the lateral superior olive. I. Sensitivity to interaural time differences. *J. Neurophysiol.* 73(3):1043–62

Julesz B. 1971. *Foundations of Cyclopean Perception*. Chicago: Univ. Chicago Press

Kapfer C, Seidl AH, Schweizer H, Grothe B. 2002. Experience-dependent refinement of inhibitory inputs to auditory coincidence-detector neurons. *Nat. Neurosci.* 5(3):247–53

Karino S, Smith PH, Yin TCT, Joris PX. 2011. Axonal branching patterns as sources of delay in the mammalian auditory brainstem: a re-examination. *J. Neurosci.* 31(8):3016–31

Klumpp RG, Eady HR. 1956. Some measurements of interaural time difference thresholds. *J. Acoust. Soc. Am.* 28(5):859–60

Kuwabara N, Zook JM. 1992. Projections to the medial superior olive from the medial and lateral nuclei of the trapezoid body in rodents and bats. *J. Comp. Neurol.* 324(4):522–38

Licklider JCR. 1948. The influence of interaural phase relations upon the masking of speech by white noise. *J. Acoust. Soc. Am.* 20:150–59

Licklider JCR. 1951. A duplex theory of pitch perception. *Experientia* 7(4):128–34

Litovsky RY, Fligor BJ, Tramo MJ. 2002. Functional role of the human inferior colliculus in binaural hearing. *Hear. Res.* 165(1–2):177–88

Louage DH, Joris PX, van der Heijden M. 2006. Decorrelation sensitivity of auditory nerve and anteroventral cochlear nucleus fibers to broadband and narrowband noise. *J. Neurosci.* 26(1):96–108

Masterton RB, Imig TJ. 1984. Neural mechanisms for sound localization. *Annu. Rev. Physiol.* 46:275–87

Masterton RB, Thompson GC, Bechtold JK, RoBards MJ. 1975. Neuroanatomical basis of binaural phase-difference analysis for sound localization: a comparative study. *J. Comp. Physiol. Psychol.* 89(5):379–86

Mc Laughlin M, Verschooten E, Joris PX. 2010. Oscillatory dipoles as a source of phase shifts in field potentials in the mammalian auditory brainstem. *J. Neurosci.* 30(40):13472–87

McAlpine D, Jiang D, Palmer A. 1996. Interaural delay sensitivity and the classification of low best-frequency binaural responses in the inferior colliculus of the guinea pig. *Hear. Res.* 97:136–52

McAlpine D, Jiang D, Palmer A. 2001. A neural code for low-frequency sound localization in mammals. *Nat. Neurosci.* 4:396–401

McCulloch WS, Pitts W. 1943. A logical calculus of the ideas immanent in nervous activity. *Bull. Math. Biophys.* 5(4):115–33

McFadden D, Pasanen EG. 1976. Lateralization at high frequencies based on interaural time differences. *J. Acoust. Soc. Am.* 59:634–39

Middlebrooks JC, Green DM. 1991. Sound localization by human listeners. *Annu. Rev. Psychol.* 42:135–59

Mills AW. 1958. On the minimum audible angle. *J. Acoust. Soc. Am.* 30(4):237–46

Moore JK, Moore RY. 1971. A comparative study of the superior olivary complex in the primate brain. *Folia Primatol.* 16(1):35–51

Myoga MH, Lehnert S, Leibold C, Felmy F, Grothe B. 2014. Glycinergic inhibition tunes coincidence detection in the auditory brainstem. *Nat. Commun.* 5:3790

Nuetzel JM, Hafter ER. 1981. Discrimination of interaural delays in complex waveforms: spectral effects. *J. Acoust. Soc. Am.* 69:1112–18

Pecka M, Brand A, Behrend O, Grothe B. 2008. Interaural time difference processing in the mammalian medial superior olive: the role of glycinergic inhibition. *J. Neurosci.* 28(27):6914–25

Plauška A, Borst JG, van der Heijden M. 2016. Predicting binaural responses from monaural responses in the gerbil medial superior olive. *J. Neurophysiol.* 115(6):2950–63

Plauška A, van der Heijden M, Borst JGG. 2017. A test of the stereausis hypothesis for sound localization in mammals. *J. Neurosci.* 37(30):7278–89

Ramón y Cajal S. 1909. *Histologie du Système Nerveux de l'Homme & des Vertébrés*. Paris: Maloine

Rautenberg PL, Grothe B, Felmy F. 2009. Quantification of the three-dimensional morphology of coincidence detector neurons in the medial superior olive of gerbils during late postnatal development. *J. Comp. Neurol.* 517(3):385–96

Rayleigh L. 1907. XII. On our perception of sound direction. *Philos. Mag.* 13:214–32

Roberts MT, Seeman SC, Golding NL. 2014. The relative contributions of MNTB and LNTB neurons to inhibition in the medial superior olive assessed through single and paired recordings. *Front. Neural Circuits* 8:49

Rose JE, Brugge JF, Anderson DJ, Hind JE. 1967. Phase-locked response to low-frequency tones in single auditory nerve fibers of the squirrel monkey. *J. Neurophysiol.* 30:769–93

Rose JE, Gross NB, Geisler CD, Hind JE. 1966. Some neural mechanisms in the inferior colliculus of the cat which may be relevant to localization of a sound source. *J. Neurophysiol.* 29:288–314

Roth GL, Kochhar RK, Hind JE. 1980. Interaural time differences: implications regarding the neurophysiology of sound localization. *J. Acoust. Soc. Am.* 68:1643–51

Sayles M, Smith PH, Joris PX. 2016. Inter-aural time sensitivity of superior-olivary-complex neurons is shaped by systematic cochlear disparities. *Assoc. Res. Otolaryngol. Abs.* 39:273

Schroeder MR. 1977. New viewpoints in binaural interactions. In *Psychophysics and Physiology of Hearing*, ed. EF Evans, JP Wilson, pp. 455–67. New York: Academic

Scott BH, Malone BJ, Semple MN. 2007. Effect of behavioral context on representation of a spatial cue in core auditory cortex of awake macaques. *J. Neurosci.* 27(24):6489–99

Scott LL, Hage TA, Golding NL. 2007. Weak action potential backpropagation is associated with high-frequency axonal firing capability in principal neurons of the gerbil medial superior olive. *J. Physiol.* 583(Pt. 2):647–61

Seidl AH, Rubel EW, Harris DM. 2010. Mechanisms for adjusting interaural time differences to achieve binaural coincidence detection. *J. Neurosci.* 30(1):70–80

Shackleton TM, Arnott RH, Palmer AR. 2005. Sensitivity to interaural correlation of single neurons in the inferior colliculus of guinea pigs. *J. Assoc. Res. Otolaryngol.* 6(3):244–59

Shamma SA, Shen NM, Gopalaswamy P. 1989. Stereausis: binaural processing without neural delays. *J. Acoust. Soc. Am.* 86(3):989–1006

Shneiderman A, Henkel CK. 1985. Evidence of collateral axonal projections to the superior olivary complex. *Hear. Res.* 19:199–205

Smith PH. 1995. Structural and functional differences distinguish principal from nonprincipal cells in the guinea pig MSO slice. *J. Neurophysiol.* 73:1653–67

Smith PH, Joris PX, Carney LH, Yin TC. 1991. Projections of physiologically characterized globular bushy cell axons from the cochlear nucleus of the cat. *J. Comp. Neurol.* 304(3):387–407

Smith PH, Joris PX, Yin TC. 1993. Projections of physiologically characterized spherical bushy cell axons from the cochlear nucleus of the cat: evidence for delay lines to the medial superior olive. *J. Comp. Neurol.* 331(2):245–60

Smith PH, Joris PX, Yin TC. 1998. Anatomy and physiology of principal cells of the medial nucleus of the trapezoid body (MNTB) of the cat. *J. Neurophysiol.* 79(6):3127–42

Spangler KM, Warr WB, Henkel CK. 1985. The projections of principal cells of the medial nucleus of the trapezoid body in the cat. *J. Comp. Neurol.* 238:249–62

Spirou GA, Berrebi AS. 1996. Organization of ventrolateral periolivary cells of the cat superior olive as revealed by PEP-19 immunocytochemistry and Nissl stain. *J. Comp. Neurol.* 368(1):100–20

Spirou GA, Berrebi AS. 1997. Glycine immunoreactivity in the lateral nucleus of the trapezoid body of the cat. *J. Comp. Neurol.* 383(4):473–88

Spirou GA, Brownell WE, Zidanic M. 1990. Recordings from cat trapezoid body and HRP labeling of globular bushy cell axons. *J. Neurophysiol.* 63:1169–90

Stern RM, Zeiberg AS, Trahiotis C. 1988. Lateralization of complex binaural stimuli: a weighted-image model. *J. Acoust. Soc. Am.* 84:156–65

Stotler WA. 1953. An experimental study of the cells and connections of the superior olivary complex of the cat. *J. Comp. Neurol.* 98:401–32

Tollin DJ. 2003. The lateral superior olive: a functional role in sound source localization. *Neuroscientist* 9(2):127–43

Tollin DJ, Yin TC. 2002. The coding of spatial location by single units in the lateral superior olive of the cat. II. The determinants of spatial receptive fields in azimuth. *J. Neurosci.* 22(4):1468–79

Tollin DJ, Yin TC. 2005. Interaural phase and level difference sensitivity in low-frequency neurons in the lateral superior olive. *J. Neurosci.* 25(46):10648–57

Tolnai S, Beutelmann R, Klump GM. 2018. Interaction of interaural cues and their contribution to the lateralisation of Mongolian gerbils (*Meriones unguiculatus*). *J. Comp. Physiol. A* 204(5):435–48

Tsuchitani C, Boudreau JC. 1966. Single unit analysis of cat superior olive S segment with tonal stimuli. *J. Neurophysiol.* 29(4):684–97

van de Par S, Trahiotis C, Bernstein LR. 2001. A consideration of the normalization that is typically included in correlation-based models of binaural detection. *J. Acoust. Soc. Am.* 109:830–33

van der Heijden M. 2018. A synaptic theory of internal delays. *J. Acoust. Soc. Am.* 144:2967–70

van der Heijden M, Joris PX. 2010. Interaural correlation fails to account for detection in a classic binaural task: dynamic ITDs dominate NoSπ detection. *J. Assoc. Res. Otolaryngol.* 11(1):113–31

van der Heijden M, Lorteije JAM, Plauška A, Roberts MT, Golding NL, Borst JGG. 2013. Directional hearing by linear summation of binaural inputs at the medial superior olive. *Neuron* 78(5):936–48

van der Heijden M, Louage DH, Joris PX. 2011. Responses of auditory nerve and anteroventral cochlear nucleus fibers to broadband and narrowband noise: implications for the sensitivity to interaural delays. *J. Assoc. Res. Otolaryngol.* 12(4):485–502

van der Heijden M, Trahiotis C. 1999. Masking with interaurally delayed stimuli: the use of "internal" delays in binaural detection. *J. Acoust. Soc. Am.* 105:388–99

Wakeford OS, Robinson DE. 1974. Lateralization of tonal stimuli by the cat. *J. Acoust. Soc. Am.* 55(3):649–52

Wallach H, Newman EB, Rosenzweig MR. 1949. The precedence effect in sound localization. *Am. J. Psychol.* 62(3):315–36

Weiss TF, Rose C. 1988. A comparison of synchronization filters in different auditory receptor organs. *Hear. Res.* 33:175–80

Yin TC, Chan JC, Carney LH. 1987. Effects of interaural time delays of noise stimuli on low-frequency cells in the cat's inferior colliculus. III. Evidence for cross-correlation. *J. Neurophysiol.* 58(3):562–83

Yin TC, Chan JK. 1990. Interaural time sensitivity in medial superior olive of cat. *J. Neurophysiol.* 64:465–88

Yin TC, Chan JK, Irvine DR. 1986. Effects of interaural time delays of noise stimuli on low-frequency cells in the cat's inferior colliculus. I. Responses to wideband noise. *J. Neurophysiol.* 55:280–300

Yin TC, Kuwada S. 1983. Binaural interaction in low-frequency neurons in inferior colliculus of the cat. III. Effects of changing frequency. *J. Neurophysiol.* 50:1020–42

Young ED, Oertel D. 2004. Cochlear nucleus. In *The Synaptic Organization of the Brain*, ed. GM Shepherd, pp. 125–63. Oxford, UK: Oxford Univ. Press

Zhou Y, Carney LH, Colburn HS. 2005. A model for interaural time difference sensitivity in the medial superior olive: interaction of excitatory and inhibitory synaptic inputs, channel dynamics, and cellular morphology. *J. Neurosci.* 25(12):3046–58

Annual Review of Neuroscience

Volume 42, 2019

Contents

Unified Classification of Molecular, Network, and Endocrine Features of Hypothalamic Neurons
Roman A. Romanov, Alán Alpár, Tomas Hökfelt, and Tibor Harkany 1

A Motor Theory of Sleep-Wake Control: Arousal-Action Circuit
Danqian Liu and Yang Dan 27

Neuronal Development of Hearing and Language: Cochlear Implants and Critical Periods
Andrej Kral, Michael F. Dorman, and Blake S. Wilson 47

Genes Involved in the Development and Physiology of Both the Peripheral and Central Auditory Systems
Nicolas Michalski and Christine Petit 67

Sodium Channels in Human Pain Disorders: Genetics and Pharmacogenomics
Sulayman D. Dib-Hajj and Stephen G. Waxman 87

Neuron-Glia Signaling in Synapse Elimination
Daniel K. Wilton, Lasse Dissing-Olesen, and Beth Stevens 107

Acoustic Pattern Recognition and Courtship Songs: Insights from Insects
Christa A. Baker, Jan Clemens, and Mala Murthy 129

Glia-Neuron Interactions in *Caenorhabditis elegans*
Aakanksha Singhvi and Shai Shaham 149

Probing Computation in the Primate Visual System at Single-Cone Resolution
A. Kling, G.D. Field, D.H. Brainard, and E.J. Chichilnisky 169

The Emerging Nature of Astrocyte Diversity
Baljit S. Khakh and Benjamin Deneen 187

Neurite Development and Repair in Worms and Flies
Claire E. Richardson and Kang Shen 209

Repeat-Associated Non-ATG Translation: Molecular Mechanisms and Contribution to Neurological Disease
Lien Nguyen, John Douglas Cleary, and Laura P.W. Ranum 227

Pathophysiology and Mechanisms of Zika Virus Infection in the Nervous System
Kimberly M. Christian, Hongjun Song, and Guo-li Ming 249

Magnetic Strategies for Nervous System Control
Michael G. Christiansen, Alexander W. Senko, and Polina Anikeeva 271

Light-Sheet Microscopy in Neuroscience
Elizabeth M.C. Hillman, Venkatakaushik Voleti, Wenze Li, and Hang Yu 295

Dexterous Hand Movements and Their Recovery After Central Nervous System Injury
Tadashi Isa 315

The Theory and Neuroscience of Cerebellar Cognition
Jeremy D. Schmahmann, Xavier Guell, Catherine J. Stoodley, and Mark A. Halko 337

Lessons from Worm Dendritic Patterning
Sharon Inberg, Anna Meledin, Veronika Kravtsov, Yael Iosilevskii, Meital Oren-Suissa, and Benjamin Podbilewicz 365

Antisense Oligonucleotide Therapies for Neurodegenerative Diseases
C. Frank Bennett, Adrian R. Krainer, and Don W. Cleveland 385

Peeling the Onion of Brain Representations
Nikolaus Kriegeskorte and Jörn Diedrichsen 407

Early Binaural Hearing: The Comparison of Temporal Differences at the Two Ears
Philip X. Joris and Marcel van der Heijden 433

What, If, and When to Move: Basal Ganglia Circuits and Self-Paced Action Initiation
Andreas Klaus, Joaquim Alves da Silva, and Rui M. Costa 459

Brainstem Circuits Controlling Action Diversification
Ludwig Ruder and Silvia Arber 485

Indexes

Cumulative Index of Contributing Authors, Volumes 33–42 505

Errata

An online log of corrections to *Annual Review of Neuroscience* articles may be found at http://www.annualreviews.org/errata/neuro